

## Semiconductor Nanocrystal Assemblies: Experimental Pitfalls and a Simple Model of Particle–Particle Interaction

Herwig Döllefeld, Horst Weller, and Alexander Eychmüller\*

*Institute for Physical Chemistry, University of Hamburg, Bundesstrasse 45, D-20146 Hamburg, Germany*

*Received: August 20, 2001; In Final Form: November 5, 2001*

Interactions in semiconductor nanocrystal assemblies have been studied on films of the cluster crystal compounds  $\text{Cd}_{17}\text{S}_4(\text{SCH}_2\text{CH}_2\text{OH})_{26}$  and  $\text{Cd}_{32}\text{S}_{14}(\text{SCH}_2\text{CH}(\text{CH}_3)\text{OH})_{36}$  prepared by spin coating. Misinterpretations of observed alterations of transition energies in these structures are avoided by the choice of an integrating sphere as the experimental setup. The resulting “real” redshift of the transition energy is explained by dipole–dipole interactions of the semiconductor nanocrystals in the films. When covalently linked, the clusters may also interact electronically.

### Introduction

Do nanocrystals interact? And if so, what is the underlying mechanism? How could we possibly observe those interactions? Several groups have raised these questions over the past years. In 1994, Vossmeier et al. studied the absorption properties of very small CdS nanoparticles.<sup>1</sup> A redshift of the first electronic transition compared to the transition observed in solution was observed when compact layers were formed from the material. Heath and co-workers published results on the behavior of metal nanoparticles arranged in a 2D monolayer using the Langmuir–Blodgett technique.<sup>2–4</sup> Small silver nanocrystals showed a shift to the red of the low energy electronic feature in a reflectance measurement when the distance between the particles is lowered. This was found valid down to a particular distance, whereas below this distance, the plasmon band disappeared because of quantum coupling. Quantum coupling of the electronic states of semiconductor quantum dots was found by Schedelbek et al.<sup>5</sup> GaAs quantum dots were prepared in a GaAlAs environment by epitaxial growth and lithographic techniques. The authors were able to prepare these dots at different distances, and quantum coupling has been proven in the photoluminescence by the observed splitting of the energy states. A very fine crystalline superstructure of CdSe nanoparticles was presented by the Bawendi group in 1995.<sup>6</sup> A comparatively small redshift could be measured in the emission spectra of the solids that was explained by small size deviations of the particles within the sample resulting in energy transfer from the smaller to the larger particles.<sup>7,8</sup> Recently, Artemyev et al. prepared unstructured solids from CdSe nanoparticles with polymers acting as spacers in order to control the distance between the particles.<sup>9,10</sup> The pure solid built up by drop casting solutions of semiconductor nanoparticles showed very broad transitions bearing resemblance with a bulk spectrum rather than with isolated absorption bands. Micic et al. obtained similar results with InP nanoparticles.<sup>11</sup> Leatherdale et al. published a paper on CdSe particles in different dielectrics.<sup>12</sup> In agreement with our results on compact layers,<sup>1</sup> a redshift of the first electronic transition was found exhibiting no significant broadening. Kim et al. presented pressure dependent studies on solutions and compact

layers of semiconductor nanoparticles.<sup>13</sup> Different stabilizing agents were used, and in contrast to the results from Leatherdale et al., no redshift was found for the compact layers of CdSe particles stabilized with trioctylphosphine/trioctylphosphineoxide (TOP/TOPO). Only for particles stabilized with pyridine was a redshift observed. Again, no significant broadening of the electronic transitions was observed. In a paper,<sup>14</sup> we presented our first results on optical studies on the cluster crystal compound  $\text{Cd}_{17}\text{S}_4(\text{SCH}_2\text{CH}_2\text{OH})_{26}$ . The structure of this thiol-stabilized molecular-like cadmium sulfide nanocrystal is known from single-crystal X-ray diffraction.<sup>15</sup> Reflection spectroscopy on micron-sized crystals yields a substantial broadening and a low energy shift of the first absorption band. In a first step, this was explained by both dipole–dipole interaction and electronic coupling of the nanocrystals in the crystalline superstructure.

In this paper, we will outline our results from studies on compact layers of very small CdS nanocrystals which will be compared to the results from the crystalline material mentioned above together with simple theoretical modeling. In addition, the necessity of preparing homogeneous layers of nanocrystals and the appropriate spectroscopy in order to gain reliable results will be outlined in detail.

### Experimental Section

**Preparation.** Cadmium sulfide particles of different sizes were prepared according to the literature.<sup>15,16</sup> In general, an alkaline aqueous solution of a cadmium salt was reacted with  $\text{H}_2\text{S}$  in the presence of an alkane thiol as the stabilizing agent. By variation of the concentrations of the precursors, the temperature, and the duration of the reaction, it was possible to control the sizes of the resulting particles. After intense dialysis, the particles were purified, and with the raising of the pH during the dialysis, the particles precipitated as white crystalline powders that can be washed with water. The powders readily redissolve in strong coordinating solvents such as dimethylformamide (DMF) or dimethyl sulfoxide. Less coordinating solvents such as alcohols or acetone are not suitable as solvents for the particles.

To obtain crystalline superstructures of the particles the dialysis was stopped after one night, and the mother liquor was kept under ambient conditions for months. Crystals up to sizes in the millimeter range were obtainable by this method.

\* To whom correspondence should be addressed. Fax: ++49-40-42838-3452. E-mail: eychmuel@chemie.uni-hamburg.de.

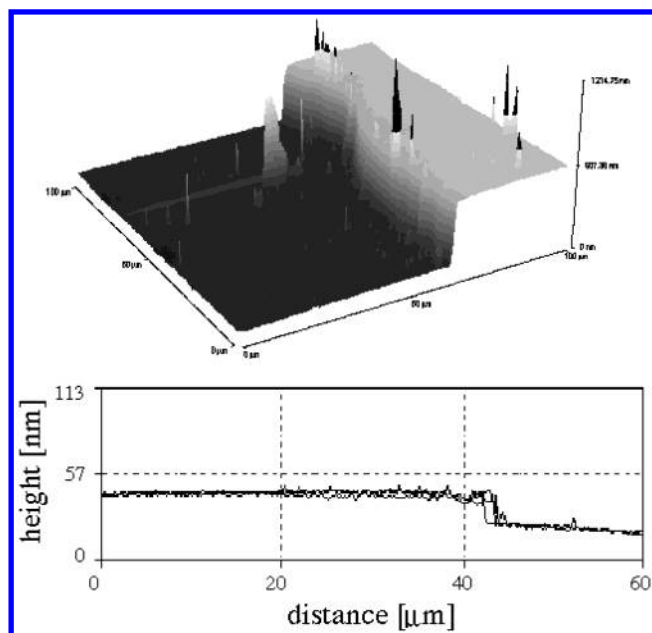


**Figure 1.** Top: Topography of a thick layer of  $\text{Cd}_{17}\text{S}_4(\text{SCH}_2\text{CH}_2\text{OH})_{26}$  particles with a thickness of about 495 nm. The obtained surface roughness for this thickness is 9 nm (1.8%, RMS). Bottom: Three AFM traces taken across a spin coated film of  $\text{Cd}_{17}\text{S}_4(\text{SCH}_2\text{CH}_2\text{OH})_{26}$  particles. The traces yield a thickness of this layer of 18.9, 21.0, and 17.2 nm, respectively. The slightly bent background underneath is explained by a drifting during the measuring process.

The particles have been characterized by different methods such as UV-vis spectroscopy, powder XRD, and single crystal XRD. The latter yields the formulas  $\text{Cd}_{17}\text{S}_4(\text{SCH}_2\text{CH}_2\text{OH})_{26}$  and  $\text{Cd}_{32}\text{S}_{14}(\text{SCH}_2\text{CH}(\text{CH}_3)\text{OH})_{36}$  for the two tetrahedral clusters with sizes of 1.4 and 1.8 nm, respectively.

**Apparatus.** UV-vis spectroscopy was performed with a Varian Cary 500 Scan spectrometer. An Ulbricht-Bowl Lab-sphere DRA-CA5500 was used as an integrating sphere. For spatially resolved UV-vis spectroscopy, a setup from Instrument Systems was used giving a lateral resolution of about 1 mm. The AFM measurements were performed with a Topometrix machine.

## Results

Compact layers were built up from concentrated solutions of the clusters in dimethylformamide (DMF) by a spin coating technique. A total of 40  $\mu\text{L}$  of cluster solution (DMF) was applied onto the quartz substrate followed by spinning of the substrate for about 1 min at 3000 rpm. After drying the sample for 1 h, a thin transparent film remained on the substrate. For controlling the content of remaining solvent and its possible dielectric influence on spectroscopic results, we compared freshly prepared layers with those that were completely dried at  $10^{-7}$  mbar for several days. No differences could be determined, the absorption spectra were absolutely identical. This procedure yields homogeneous layers of nanocrystals on quartz substrates. We used the spin coating technique in order to avoid sample inhomogeneities which are obtained by simply evaporating the solvent. The homogeneity of the films was seen by taking UV-vis absorption spectra on five different spots on the quartz plates. The spectra were absolutely identical as opposed to samples that were built up by drop casting of a colloidal solution. The homogeneity of these layers is also seen by AFM (Figure 1). The upper image shows the topography of a thick layer with a thickness of about 495 nm. The spikes are attributed to recording artifacts. The lower image shows three

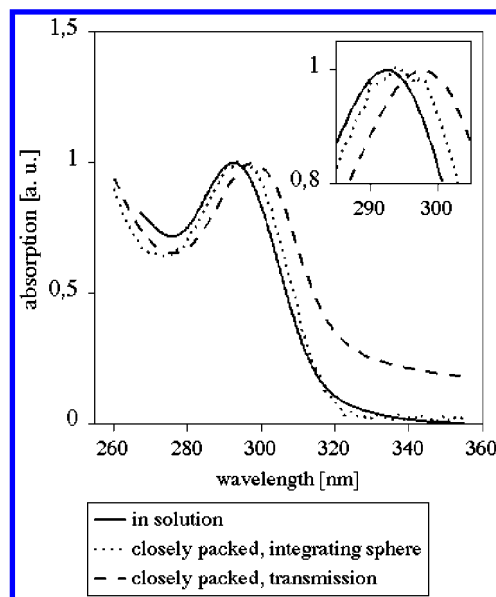


**Figure 2.** Absorption spectra of a compact layer of  $\text{Cd}_{17}\text{S}_4(\text{SCH}_2\text{CH}_2\text{OH})_{26}$  nanoparticles in comparison to the spectrum of the same particles in solution (solid line). Significant scattering is observed when the layer is measured in transmission geometry (dashed line) instead of measuring in the integrating sphere (dotted line). The inset provides a closer look on the resulting changes in the position of the maximum of the transition band depending on the experimental setup. (solution: cell thickness = 1 cm, OD = 1.15, calculated concentration = 0.7  $\mu\text{mol/L}$ ; integrating sphere: OD = 0.14, calculated film thickness = 30 nm; transmission: OD = 0.26, calculation of film thickness difficult because of scattering background, estimated to be 25 nm)

traces across a rather thin layer of about 19 nm. Even for such samples, it seems that very uniform layers have been obtained. The thickness of the layers could easily be controlled by varying the concentrations in the solutions. Most probably, the viscosity of the solutions determined the resulting thickness of the layers. Also, the thickness was measured with the AFM, resulting in a linear dependence of the optical density on the thickness of the layers.

The films were stable in air for at least six months. Only in the very thin samples was slow degradation probably at the surface of the layers observed.

The electronic properties of the nanocrystals in the films were determined by measuring the absorption in the UV-vis region. Figure 2 shows absorption spectra of a compact layer of  $\text{Cd}_{17}\text{S}_4(\text{SCH}_2\text{CH}_2\text{OH})_{26}$  nanocrystals taken in transmission geometry (dashed line) together with the spectrum of the isolated clusters in solution (solid line). The spectrum of the compact layer was found to be shifted to the red. In addition, we found that the absorption band of the first electronic transition was clearly resolved and was not broadened significantly. Surprisingly, the absolute value of the redshift varied with the thickness of the compact layer. The maximum of the redshift in comparison to the spectra of the clusters in solution was about 70 meV at an optical density of about 0.1 at the absorption maximum.

Although the compact layers appear totally transparent in the visible region, a scattering background is seen in the spectra of compact layers (cf., e.g., Figure 2, dashed line). To avoid any measuring artifacts in the experiment, an integrating sphere was used. The absorption measurement of the same layer in this different setup resulted in significantly different signals, i.e., in the removal of the scattering background (dotted line in Figure 2). Furthermore, the spectrum remains redshifted in comparison to the solution spectrum but by a smaller number than deduced

**TABLE 1: Redshift of the First Electronic Transition of Compact Layers of CdS Nanocrystals in Comparison to the Corresponding Transition of the Same Clusters in Solution<sup>a</sup>**

cluster sizes	experimental $\Delta E$ [meV]	calculated spherical $\Delta E$ [meV]	calculated tetrahedral $\Delta E$ [meV]
$d = 1.8$ nm	12	27.2	6.7
$d = 1.4$ nm	29	51.2	14.2

<sup>a</sup> Shown are the experimental values for the different cluster sizes as well as the calculated results. The theoretical results for both spherically or tetrahedrally shaped particles are given. Note that for both particle sizes the experimental value fits between the values of the assumed particle shapes.

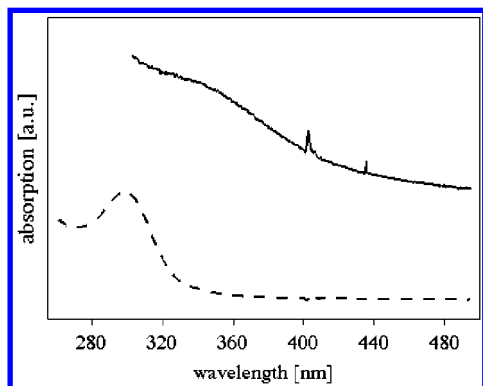


**Figure 3.** Absorption spectra of a sample of  $\text{Cd}_{17}\text{S}_4(\text{SCH}_2\text{CH}_2\text{OH})_{26}$  nanocrystals prepared by dropcasting taken at a “good” spot (dashed line) and a “bad” spot (solid line).

before. Additionally, the measurement in the integrating sphere did not show anymore a dependence on the thickness of the layers. Thus, regarding the discussion of the energetic position of an absorption band, it is extremely important to suppress artifacts caused by scattering. Keeping this in mind, we observed a redshift of the first electronic transition in the compact layer of about 29 meV in comparison to the isolated cluster in solution.

After having evaluated appropriate preparation techniques of compact films of high quality and reproducibility together with the measuring conditions in an integrating sphere we examined clusters of different sizes. The spectra of the compact layers of the two cluster compounds showed a significant redshift of the first electronic transition compared to the corresponding spectra of the clusters in solution. The amount of the shift depends on the cluster size: the smaller the clusters, the larger the shift. Table 1 shows the exact numbers of the redshifts obtained for the two cluster compounds. The redshift for the larger cluster ( $\phi = 1.8$  nm) amounts to 12 meV which transforms to 1 nm in the energy range of 330 nm.

## Discussion

As pointed out in the preceding section, a proper film preparation is essential for the study of particle–particle interactions in semiconductor nanocrystal assemblies. As an illustration of this in Figure 3, we show some results from an erroneous experiment: a drop of a colloidal solution of  $\text{Cd}_{17}\text{S}_4(\text{SCH}_2\text{CH}_2\text{OH})_{26}$  nanocrystals in DMF has been dried on a quartz substrate under ambient conditions. The two spectra seen in Figure 3 have been taken from different spots of this sample appearing clearly different. Whereas the dashed line resembles the proper spectra shown in Figure 2, the solid line leads to false conclusions. Namely, when the scattering background is neglected, a bulklike absorption seems to occur in the nanocrystal solid.

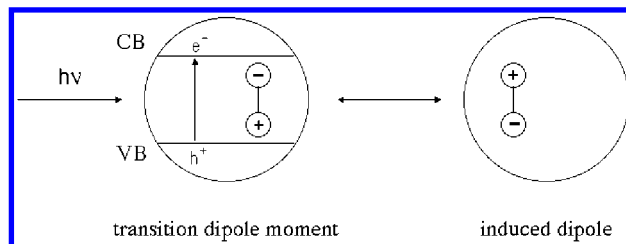


**Figure 4.** Schematic view of the interaction of the transition dipole moment of a particle and the induced dipole moment of a neighboring particle.

We will now outline some thoughts regarding the understanding of the observed redshifts in nanocrystal films. For explaining the experimental results, we would like to introduce a simple model in order to estimate the influence of the polar properties of the surrounding medium on the transition energy. In this model, the transition dipole moment of the light absorbing particle may induce dipole moments in the neighboring particles in their ground state. Figure 4 shows schematically the interacting components, i.e., the interaction between the transition dipole moment of the absorbing particle and the induced dipole moments in the neighboring particles. Analogous to the additional coulomb term in the Brus formula,<sup>17</sup> this interaction between the dipoles could lower the initial transition energy. For our calculations, we obtained the oscillator strength  $f$  of the transition from spectroscopic data and evaluated the transition dipole moment using textbook equations:

$$f = 4.3 \times 10^{-9} \int \epsilon \, d\tilde{\nu} \approx 4.3 \times 10^{-9} \cdot \epsilon_{\text{max}} \cdot \text{fwhm}$$

and the transition dipole moment  $\mu_{\text{tr}}$  of the absorption process

$$\mu_{\text{tr}} = \sqrt{\frac{3\hbar e^2}{8\pi^2 m_e \nu_{\text{max}}}} f = \sqrt{2.15 \times 10^6 \frac{f}{\tilde{\nu}}}$$

with the absorption coefficient  $\epsilon$ , the wavenumber  $\tilde{\nu}$  [ $\text{cm}^{-1}$ ], the full width at half-maximum fwhm [ $\text{cm}^{-1}$ ], Planck’s constant  $\hbar$ , the elementary charge  $e$ , and the effective mass of the electron  $m_e$ . If it is supposed that the formula of Clausius and Mossotti is appropriate in this case, then the polarizability volume of the clusters was calculated from the bulk high-frequency dielectric constant ( $\epsilon = 5.5$ ) by

$$\alpha' = \left( \frac{\epsilon - 1}{\epsilon + 2} \right) \cdot \frac{3\epsilon_0}{N} \frac{1}{4\pi\epsilon_0} \approx 0.6V \frac{3}{4\pi} = 0.6r^3$$

with the particle density  $N$ , the volume  $V$ , and the radius  $r$ . Although this value could be altered for small particles, it is quite common to use the bulk value for a first rough estimate (see, e.g., ref 17). The potential energy of the interaction between a dipole moment and an induced dipole moment is given by<sup>18</sup>

$$E_{\text{pot}} = -\frac{\mu_1^2 \alpha'_2}{\pi\epsilon_0 r^6}$$

For the 1.4 nm particle, we obtained a value for the oscillator strength close to one which is expected for this kind of molecular species having nearly perfect overlap of the wave functions of the charge carriers. The resulting transition dipole moment amounts to 7.9 D which fits nicely in the linear dependence of the dipole moments on the cluster sizes found by others.<sup>19–25</sup> The resulting polarizabilities strongly depend on the assumed particle shapes and volumes. Assuming a spherical shape with



a diameter of 1.4 nm, we obtained a polarizability volume of  $205.8 \text{ \AA}^3$ . For a distance between the particles (center to center) of 1.4 nm, this yields a potential energy of  $-51.2 \text{ meV}$  for the interaction between the dipole of the absorbing cluster and the induced dipoles in adjacent clusters (cf. Table 1). If we take the polarizability volume of the intact tetrahedrally shaped particles ( $57.0 \text{ \AA}^3$ ), a shift of  $-14.2 \text{ meV}$  to lower energies arises from the calculation. Comparing these results with the value of the experiment ( $-29 \text{ meV}$ ), these simple calculations explain the redshift of the absorption band of the clusters in the compact layer in comparison to the isolated clusters in solution quite well.

In Table 1, the experimental results for the particles with sizes of 1.4 and 1.8 nm are shown together with the calculated data. For both particle sizes, the experimental results are found to lie between the calculated values for spheres and tetrahedra, respectively.

As mentioned above, other groups discuss the energy shift of the first electronic transition in the absorption spectra by polarization effects because of changes in the dielectric properties of the surrounding environment, sometimes called "solvatochromism".<sup>12,13,26,27</sup> This effect being relevant for semiconductor particles was first discussed by Brus.<sup>28</sup> Recently, Brus and co-workers presented a theoretical study on CdSe nanoparticles<sup>26</sup> based on a modified pseudopotential method. The calculations yielded large dipole moments of the nanocrystals resulting from the anisotropy of the crystal structure of hexagonal cadmium selenide particles. Those moments are affected by a polar environment. However, the authors propose only weak interactions with a polar environment for particles from materials with isotropic crystal structure like cubic cadmium sulfide which is the substance of our investigations.

Leatherdale et al. explained the observed small redshift (4 meV) of the absorption band in their experiment on CdSe particles stabilized by TOP/TOPO by the polarization energy including screening within a core-shell model<sup>12</sup> (and references therein). Opposed to these results Kim et al. exclude an influence of the dielectric surrounding on the first electronic transition of their CdSe nanocrystals if they also were stabilized with TOP/TOPO.<sup>13</sup> A shift of about 25 meV has been observed by these authors for the system CdSe capped with pyridine. Thus, whether in CdSe stabilized by TOP/TOPO a significant redshift is observed may depend on the individual viewpoint. However, we applied our simple model to the CdSe particles ( $\phi = 4 \text{ nm}$ ) mentioned above by Leatherdale and co-workers. With  $\epsilon = 6.2$ ,  $\text{fwhm} = 936 \text{ cm}^{-1}$ ,  $\tilde{\nu} = 17\,812 \text{ cm}^{-1}$ ,<sup>12</sup> and  $\epsilon_{\text{max}} = 200\,000 \text{ l mol}^{-1} \text{ cm}^{-1}$ ,<sup>29</sup> we obtained an oscillator strength of  $f = 0.81$ , a transition dipole moment of  $\mu_{\text{tr}} = 9.86 \text{ D}$ , and a polarizability volume of  $\alpha' = 5073 \text{ \AA}^3$ . With these numbers, the calculated redshift amounts to 3.6 meV which fits very nicely to the experimental result from Leatherdale et al. (4 meV).

Both descriptions, our model of dipole-dipole interaction and that focusing on the polarization energy, consider the dielectric properties of the surrounding environment. The formalism introduced by Brus and cited by many other groups focuses on the dielectric properties of a continuous medium around the particles. An advantage of our model introduced above taking into account the coupling of discrete dipoles of neighboring particles seems to be its simplicity. Only textbook equations are used with very little calculational expenditure. The results are in fair agreement with the obtained experimental values for the redshift of the first electronic transition.

For the remainder of this paper, we will try to shed some light on yet another mechanism of interaction in quantum dot

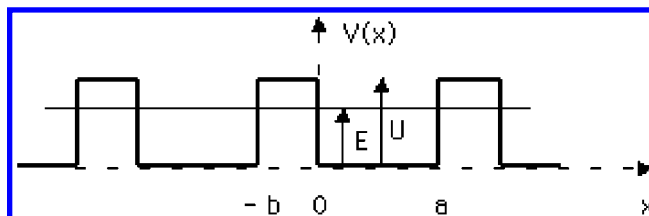


**Figure 5.** 1D periodic box potential according to Kronig and Penney with the width of the boxes  $a$  representing the diameter of the particles and the width  $b$  and height  $U$  of the energy barrier. The width of the barrier represents the distance between the particles. The energy level  $E$  for the resulting delocalized electronic system is plotted schematically as well.

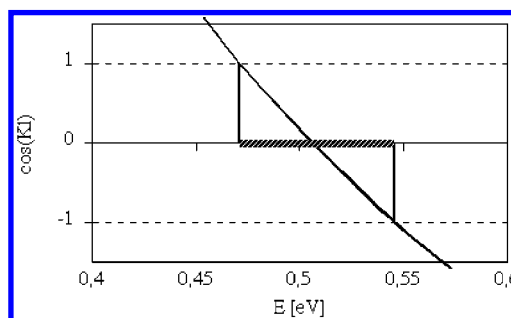


**Figure 6.** Graphic solution from the model of Kronig and Penney for the energy states of the electron in a nanoparticle with a small distance between the particles (for details of the calculation see text). The boundary conditions for the wave function yield an expression including a cosine function with the wavevector  $K$  and the period length  $l$  ( $l = a + b$ , cf. Figure 5). The cosine function values (between 1 and  $-1$ ) yield the permitted energy region for the electronic states. In this case, this is a subband spreading over 75 meV.

solids. To the best of our knowledge, the results presented in our previous paper<sup>14</sup> are the only published work thus far on the energetic position of the first electronic transition in a crystalline superstructure made from nanocrystals. These crystals of very small CdS nanoparticles of the composition  $\text{Cd}_{17}\text{S}_{4}(\text{SCH}_2\text{CH}_2\text{OH})_{26}$  were prepared as described above. We showed that the first electronic transition is shifted to the red in comparison to the solution by about 150 meV and the transition is significantly broadened.<sup>14</sup> Thus, the shift in the crystalline material is larger (150 meV compared to 29 meV in the films), and in addition to the shift, a broadening of the absorption band is observed being absent in the nanocrystal films. For the larger redshift, a more densely packed structure of the crystals compared to the films is held responsible, whereas for the broadening, we propose a model of quantum mechanical coupling. For calculating the dependence of the electronic interaction on the distance between the coupling systems, we used the periodical box potential shown in Figure 5 according to Kronig and Penney<sup>30</sup> for simulating both the crystalline arrangement of the particles with very small distances between them and the situation in solution with large distances between the particles. In this model, the boxes representing the particles (size 1.4 nm) are separated by potential walls. The height of these energy barriers was chosen to be 3 eV, and the separation of the boxes (i.e., the interparticle distance) was varied between 20 nm reflecting large distances and 0.7 nm modeling the situation with neighboring clusters. The effective masses of the charge carriers were taken from the literature (0.2 and 0.7 for electrons and holes, respectively<sup>31</sup>). The 3D arrangement of the particles was taken into account by multiplying the 1D results by three. According to Brus,<sup>17</sup> the transition energy then is calculated by addition of the bulk band gap and the Coulomb interaction. For large distances between the clusters a transition

energy of 3.92 eV was obtained which is in fair agreement of the experimental value (4.24 eV). For the clusters with small distances between the inorganic cores (0.7 nm), we obtained the formation of a subband for the electron states which spans about 75 meV (for 1D, Figure 6). Because of the larger effective mass of the holes, a narrower subband (1.5 meV) is observed for this charge carrier. The centers of the subbands remain exactly at the same energetic positions as the discrete levels in the solution case. Thus, it turns out that for the electronic interaction of semiconductor particles in close contact a broadening of the transition band is expected without a significant change of the transition energy. The shift of the transition energy in the crystalline material is then due only to dipole–dipole interactions of adjacent particles.

**Acknowledgment.** We thank Dr. Andreas Richter, Institut für Angewandte Physik, Universität Hamburg, for performing the AFM measurements. This work was supported by the Deutsche Forschungsgemeinschaft, Sonderforschungsbereich 508.

## References and Notes

- (1) Vossmeier, T.; Katsikas, L.; Giersig, M.; Popovic, I. G.; Diesner, K.; Chemseddine, A.; Eychmüller, A.; Weller, H. *J. Phys. Chem.* **1994**, *98*, 7665.
- (2) Collier, C. P.; Saykally, R. J.; Shiang, J. J.; Heinrichs, S. E.; Heath, J. R. *Science* **1997**, *277*, 1978.
- (3) Shiang, J. J.; Heath, J. R.; Collier, C. P.; Saykally, R. J. *J. Phys. Chem. B* **1998**, *102*, 3425.
- (4) Collier, C. P.; Vossmeier, T.; Heath, J. R. *Annu. Rev. Phys. Chem.* **1998**, *49*, 371.
- (5) Schedelbeck, G.; Wegschneider, W.; Bichler, M.; Abstreiter, G. *Science* **1997**, *278*, 1792.
- (6) Murray, C. B.; Kagan, C. R.; Bawendi, M. G. *Science* **1995**, *270*, 1335.
- (7) Kagan, C. R.; Murray, C. B.; Nirmal, M.; Bawendi, M. G. *Phys. Rev. Lett.* **1996**, *76*, 1517.
- (8) Kagan, C. R.; Murray, C. B.; Bawendi, M. G. *Phys. Rev. B* **1996**, *54*, 8633.
- (9) Artemyev, M. V.; Bibik, A. I.; Gurinovich, L. I.; Gaponenko, S. V.; Woggon, U. *Phys. Rev. B* **1999**, *60*, 1504.
- (10) Artemyev, M. V.; Woggon, U.; Jaschinski, H.; Gurinovich, L. I.; Gaponenko, S. V. *J. Phys. Chem.* **2000**, *104*, 11617.
- (11) Micic, O. I.; Ahrenkiel, S. P.; Nozik, A. *Appl. Phys. Lett.* **2001**, *78*, 4022.
- (12) Leatherdale, C. A.; Bawendi, M. G. *Phys. Rev. B* **2001**, *63*, 165315.
- (13) Kim, B. S.; Islam, M. A.; Brus, L. E.; Herman, I. P. *J. Appl. Phys.* **2001**, *89*, 8127.
- (14) Döllefeld, H.; Weller, H.; Eychmüller, A. *Nano Lett.* **2001**, *1*, 267.
- (15) Vossmeier, T.; Reck, G.; Katsikas, L.; Haupt, E. T. K.; Schulz, B.; Weller, H. *Science* **1995**, *267*, 1476.
- (16) Vossmeier, T.; Reck, G.; Schulz, B.; Katsikas, L.; Weller, H. *J. Am. Chem. Soc.* **1995**, *117*, 12881.
- (17) Brus, L. E. *J. Chem. Phys.* **1984**, *80*, 4403.
- (18) Atkins, P. A. *Physikalische Chemie*, 2. Auflage, German Edition ed.; VCH Verlagsgesellschaft: Weinheim, Germany, 1996.
- (19) Colvin, V. L.; Alivisatos, A. P. *J. Chem. Phys.* **1992**, *97*, 730.
- (20) Colvin, V. L.; Cunningham, K. L.; Alivisatos, A. P. *J. Chem. Phys.* **1994**, *101*, 7122.
- (21) Blanton, S. A.; Leheny, R. L.; Hines, M. A.; Guyot-Sionnest, P. *Phys. Rev. Lett.* **1997**, *79*, 865.
- (22) Empedocles, S. A.; Bawendi, M. G. *Science* **1997**, *278*, 2114.
- (23) Empedocles, S. A.; Neuhauser, R.; Bawendi, M. G. *Nature* **1999**, *399*, 126.
- (24) Empedocles, S. A.; Neuhauser, R.; Shimizu, K.; Bawendi, M. G. *Adv. Mater.* **1999**, *11*, 1243–1256.
- (25) Shim, M.; Guyot-Sionnest, P. *J. Chem. Phys.* **1999**, *111*, 6955.
- (26) Rabani, E.; Hetenyi, B.; Berne, B. J.; Brus, L. E. *J. Chem. Phys.* **1999**, *110*, 5355.
- (27) Banyai, L.; Gilliot, P. *Phys. Rev. B* **1992**, *45*, 14136.
- (28) Brus, L. E. *J. Chem. Phys.* **1983**, *79*, 5566.
- (29) Schmelz, O.; Mews, A.; Basché, T.; Herrmann, A.; Müllen, K. *Langmuir* **2001**, *17*, 2861.
- (30) Flügge, S. *Rechenmethoden der Quantentheorie*, 5. verbesserte Auflage; Springer-Verlag: Berlin, Germany, 1993.
- (31) *Landolt-Börnstein Numerical Data and Functional Relationship in Science and Technology*; Springer-Verlag: Berlin, Germany 1982; Vol. New Series, Group III, 22 a, Section 3.6.